View metadata, citation and similar papers at core.ac.uk

brought to you by CORE

provided by epublications@Marquette

Marquette University
e-Publications@Marquette

Chemistry Faculty Research and Publications | Chemistry, Department of

5-1-2016

The Use of Isomeric Testosterone Dimers to Explore Allosteric Effects in Substrate Binding to Cytochrome P450 CYP3A4

Ilia G. Denisov
University of Illinois at Urbana-Champaign

Piotr J. Mak
Marquette University, piotr.mak@marquette.edu

Yelena V. Grinkova
University of Illinois at Urbana-Champaign

Dominic Bastien
Université du Québec à Trois-Rivières

Gervais Bérubé
Université du Québec à Trois-Rivières

See next page for additional authors

Accepted version. *Journal of Inorganic Biochemistry*, Vol. 158 (May 2016): 77-85. DOI. © 2015 Elsevier Inc. Used with permission.
NOTICE: this is the author's version of a work that was accepted for publication in *Journal of Inorganic Biochemistry*. Changes resulting from the publishing process, such as peer review, editing, corrections, structural formatting, and other quality control mechanisms may not be reflected in this document. Changes may have been made to this work since it was submitted for publication. A definitive version was subsequently published in *Journal of Inorganic Biochemistry*, Vol. 158 (May 2016): 77-85. DOI.

Authors
Ilia G. Denisov, Piotr J. Mak, Yelena V. Grinkova, Dominic Bastien, Gervais Bérubé, Stephen G. Sligar, and James R. Kincaid

This article is available at e-Publications@Marquette: http://epublications.marquette.edu/chem_fac/450

***NOT THE PUBLISHED VERSION;* this is the author's final, peer-reviewed manuscript.** The published version may be accessed by following the link in the citation at the bottom of the page.

The Use of Isomeric Testosterone Dimers to Explore Allosteric Effects in Substrate Binding to Cytochrome P450 CYP3A4

Ilia G. Denisov
Department of Biochemistry, University of Illinois, Urbana, IL
Piotr J. Mak
Department of Chemistry, Marquette University, Milwaukee, WI
Yelena V. Grinkova
Department of Biochemistry, University of Illinois, Urbana, IL
Dominic Bastien
Département de chimie, biochimie et physique, Université du Québec à Trois-Rivières, Trois-Rivières, Québec G9A 5H7, Canada
Gervais Bérubé
Département de chimie, biochimie et physique, Université du Québec à Trois-Rivières, Trois-Rivières, Québec G9A 5H7, Canada

Journal of Inorganic Biochemistry, Vol 158, (May 2016): pg. 77-85. DOI. This article is © Elsevier and permission has been granted for this version to appear in e-Publications@Marquette. Elsevier does not grant permission for this article to be further copied/distributed or hosted elsewhere without the express permission from Elsevier.

***NOT THE PUBLISHED VERSION;* this is the author's final, peer-reviewed manuscript.** The published version may be accessed by following the link in the citation at the bottom of the page.

Stephen G. Sligar

Department of Biochemistry and Department of Chemistry,
University of Illinois,
Urbana, IL

James R. Kincaid

Department of Chemistry, Marquette University,
Milwaukee, WI

Abstract: Cytochrome P450 CYP3A4 is the main drug-metabolizing enzyme in the human liver, being responsible for oxidation of 50% of all pharmaceuticals metabolized by human P450 enzymes. Possessing a large substrate binding pocket, it can simultaneously bind several substrate molecules and often exhibits a complex pattern of drug–drug interactions. In order to better understand structural and functional aspects of binding of multiple substrate molecules to CYP3A4 we used resonance Raman and UV–VIS spectroscopy to document the effects of binding of synthetic testosterone dimers of different configurations, *cis*-TST_2 and *trans*-TST_2. We directly demonstrate that the binding of two steroid molecules, which can assume multiple possible configurations inside the substrate binding pocket of monomeric CYP3A4, can lead to active site structural changes that affect functional properties. Using resonance Raman spectroscopy, we have documented perturbations in the ferric and Fe-CO states by these substrates, and compared these results with effects caused by binding of monomeric TST. While the binding of *trans*-TST_2 yields results similar to those obtained with monomeric TST, the binding of *cis*-TST_2 is much tighter and results in significantly more pronounced conformational changes of the porphyrin side chains and Fe-CO unit. In addition, binding of an additional monomeric TST molecule in the remote allosteric site significantly improves binding affinity and the overall spin shift for CYP3A4 with *trans*-TST_2 dimer bound inside the substrate binding pocket. This result provides the first direct evidence for an allosteric effect of the peripheral binding site at the protein-membrane interface on the functional properties of CYP3A4.

Graphical abstract: Synthetic dimers of the steroid testosterone are used to address directly the mechanisms of multiple substrate binding at the active site of cytochrome P450 3A4 and the role of substrate binding at a distal site in the control of allostery in this central enzyme of human drug metabolism.

Journal of Inorganic Biochemistry, Vol 158, (May 2016): pg. 77-85. DOI. This article is © Elsevier and permission has been granted for this version to appear in e-Publications@Marquette. Elsevier does not grant permission for this article to be further copied/distributed or hosted elsewhere without the express permission from Elsevier.

***NOT THE PUBLISHED VERSION;* this is the author's final, peer-reviewed manuscript.** The published version may be accessed by following the link in the citation at the bottom of the page.

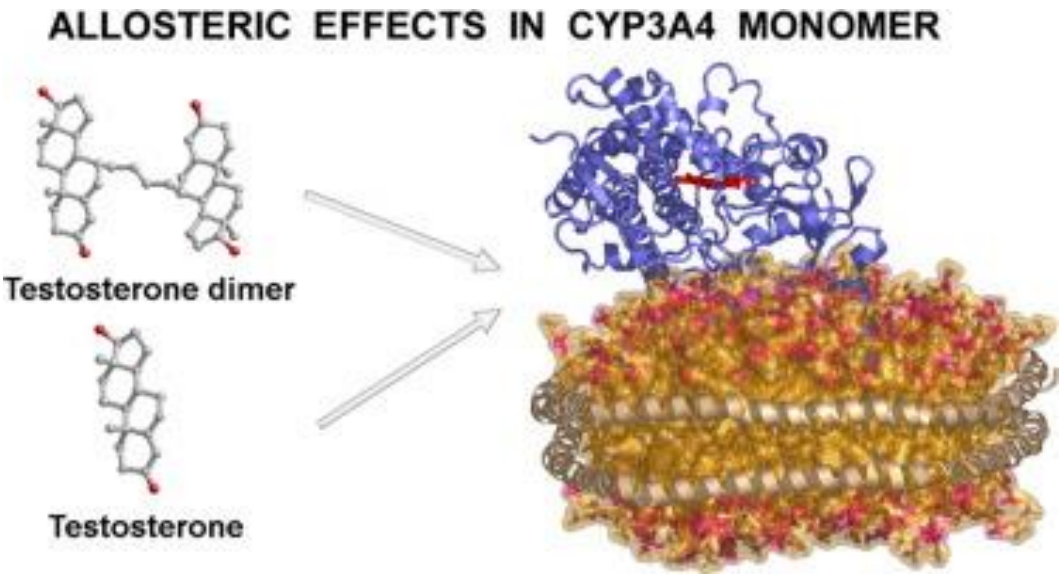

Keywords: Cytochrome P450, CYP3A4, Resonance Raman, Allosteric properties, Nanodiscs, Testosterone dimers

1. Introduction

CYP3A4 is the most abundant xenobiotic metabolizing cytochrome P450 in humans. It is responsible for the metabolism of approximately half of the drugs metabolized by P450 enzymes[1] and as such affords unusually broad substrate specificity, with the substrate size spanning from ethanol (46 Da) to cyclosporine (1202 Da).[2] Given its large and malleable substrate binding pocket, CYP3A4 can simultaneously bind several substrate molecules, often exhibiting substantial deviations from the simple Michaelis–Menten kinetics of enzymatic catalysis owing to homotropic or heterotropic cooperative interactions. Attaining a detailed mechanistic understanding of these interactions is important for the problem of drug–drug interactions mediated by cytochromes P450,[3] a critical issue for development and clinical trials of new pharmaceutical compounds. Various approaches to this problem have been described previously,[3,4,5,6,7,8,9] but no detailed molecular picture has yet emerged to help resolve the pressing need to better understand drug–drug interactions mediated by CYP3A4 or other important drug-metabolizing cytochromes P450, such as CYP2C9 and CYP2D6.

Journal of Inorganic Biochemistry, Vol 158, (May 2016): pg. 77-85. DOI. This article is © Elsevier and permission has been granted for this version to appear in e-Publications@Marquette. Elsevier does not grant permission for this article to be further copied/distributed or hosted elsewhere without the express permission from Elsevier.

***NOT THE PUBLISHED VERSION;* this is the author's final, peer-reviewed manuscript.** The published version may be accessed by following the link in the citation at the bottom of the page.

Recently we developed a new method for deciphering the cooperative interactions of various substrates with CYP3A4, which is based on the global analysis of multiple experimental data sets obtained under identical conditions. This was accomplished using functionally competent reconstituted assemblies of CYP3A4 with P450 reductase incorporated into Nanodiscs.[10] Using testosterone (TST) as a model substrate, we were able to resolve the experimentally observed functional properties as a function of the substrate concentration and proved that at least three TST molecules can bind to each monomeric CYP3A4 Nanodisc assembly; i.e., ND:CYP3A4. The resolved stepwise stoichiometric dissociation constants (19, 37, and 56 μM) reveal that virtually no specific cooperative interactions between substrate binding sites is present (the cooperative free energy being estimated as less than 0.5 kcal/mol). Rather, the well-known non-Michaelis–Menten kinetics of TST hydroxylation by CYP3A4 is due to the different functional properties of the enzyme carrying one, two, or three substrates. While binding of the first TST molecule does not result in any product formation, the second binding event turns on the full catalytic activity of the enzyme and the third binding step significantly improves the efficiency of CYP3A4 catalysis, with fewer redox equivalents being consumed per one productive turnover.[10]

However, although the above referenced efforts have provided thorough documentation of functional properties, the structural basis for such complex effects caused by interactions of multiple steroid molecules with CYP3A4 remains obscure. Currently there are two X-ray structures of CYP3A4 with two organic molecules inside the substrate binding pocket, but both represent Type II inhibitors with one molecule coordinating to the heme iron as the sixth axial ligand, while another packs on the side[11] or on top[12] of the first. The only structure of CYP3A4 with steroid progesterone bound as a substrate reveals a peripheral binding site on the outside of the F-F′ and G-G′ loops.[13] Recent efforts to crystallize CYP3A4 occupied with a specified number of progesterone molecules also ended with the structures with only one steroid molecules at the peripheral site,[14] very similar to the one reported earlier. This result confirms that obtaining crystals of CYP3A4 with a given number of substrate molecules presents difficult challenges. In addition, crystallization of cytochromes P450 is currently accomplished only using soluble forms of these monotopic membrane proteins, with no lipid bilayer present. Thus, more information about

Journal of Inorganic Biochemistry, Vol 158, (May 2016): pg. 77-85. DOI. This article is © Elsevier and permission has been granted for this version to appear in e-Publications@Marquette. Elsevier does not grant permission for this article to be further copied/distributed or hosted elsewhere without the express permission from Elsevier.

***NOT THE PUBLISHED VERSION;* this is the author's final, peer-reviewed manuscript.** The published version may be accessed by following the link in the citation at the bottom of the page.

the positioning of two steroid molecules inside the substrate binding pocket of CYP3A4 and their mutual interactions resulting in the functionally active enzyme-substrate complex, can most conveniently be obtained using spectroscopic methods using CYP3A4 incorporated into the Nanodisc lipid bilayer while the high affinity binding site for steroids in CYP3A4 is most likely located at the protein-membrane interface.[15]

Recently we have published a thorough comparison of CYP3A4 interacting with several substrates, including erythromycin, bromocryptine and TST, using resonance Raman (rR) spectroscopy[16] to acquire high quality spectra for the ferric form and the ferrous CO adducts. Various perturbations of the vibrational modes of the heme and the internal modes of the Fe-CO fragment provided useful insight into the active site structural changes imposed by binding erythromycin, bromocryptine or saturating amounts of TST. Indeed, these studies suggested, among other useful facts, that binding of bromocryptine within the CYP3A4 substrate pocket induced functionally significant out-of-plane distortion of the heme plane and vinyl group disposition that was only later confirmed by crystallographic studies.[17] However, because of the essentially non-cooperative binding of TST to CYP3A4 and strong overlap of population distributions of CYP3A4 binding intermediates with one, two or three bound TST molecules, it was impossible to confidently assign the observed rR spectral changes to a particular binding event so as to allow for definitive structural interpretation. Fortunately, the nearly coincident report of the synthesis of TST dimers of different configurations[18] opened a new opportunity for the spectroscopic study of possible binding modes of steroids by CYP3A4, the results of which are reported herein.

The essential advantage of these TST dimers is that comparison of the rR spectra of CYP3A4 in the presence of dimers with known spatial structures can remove the ambiguity of the earlier work, helping to remove the heterogeneity of the system and overlap of signals from multiple binding intermediates. Owing to the large size of TST dimers we expect their binding to CYP3A4 to follow a simple 1:1 stoichiometry, resulting in much better characterized CYP3A4 complexes with two TST molecules packed inside the substrate binding pocket with different configurations. Specifically, in *cis*-TST the two

Journal of Inorganic Biochemistry, Vol 158, (May 2016): pg. 77-85. DOI. This article is © Elsevier and permission has been granted for this version to appear in e-Publications@Marquette. Elsevier does not grant permission for this article to be further copied/distributed or hosted elsewhere without the express permission from Elsevier.

***NOT THE PUBLISHED VERSION;* this is the author's final, peer-reviewed manuscript.** The published version may be accessed by following the link in the citation at the bottom of the page.

steroid moieties are positioned one on top of the other in almost parallel orientation, while in *trans*-TST they are separated in space (Fig. 1), so that the binding in CYP3A4 is expected to position one steroid near the heme iron with the second one extended towards the entrance to the binding pocket. Comparison of the spectral characteristics of these two CYP3A4–TST dimer complexes with those of the previously measured CYP3A4 complexes with monomeric TST provides information regarding steroid binding modes to CYP3A4. In addition, titration experiments with mixtures of *trans*-TST_2 dimer with TST monomer help reveal the role of the allosteric remote binding site[7,14,15,19,20,21] in steroid binding to CYP3A4 monomer incorporated in the 1-palmitoyl-2-oleoyl-sn-glycero-3-phosphocholine (POPC) lipid bilayer of Nanodiscs.

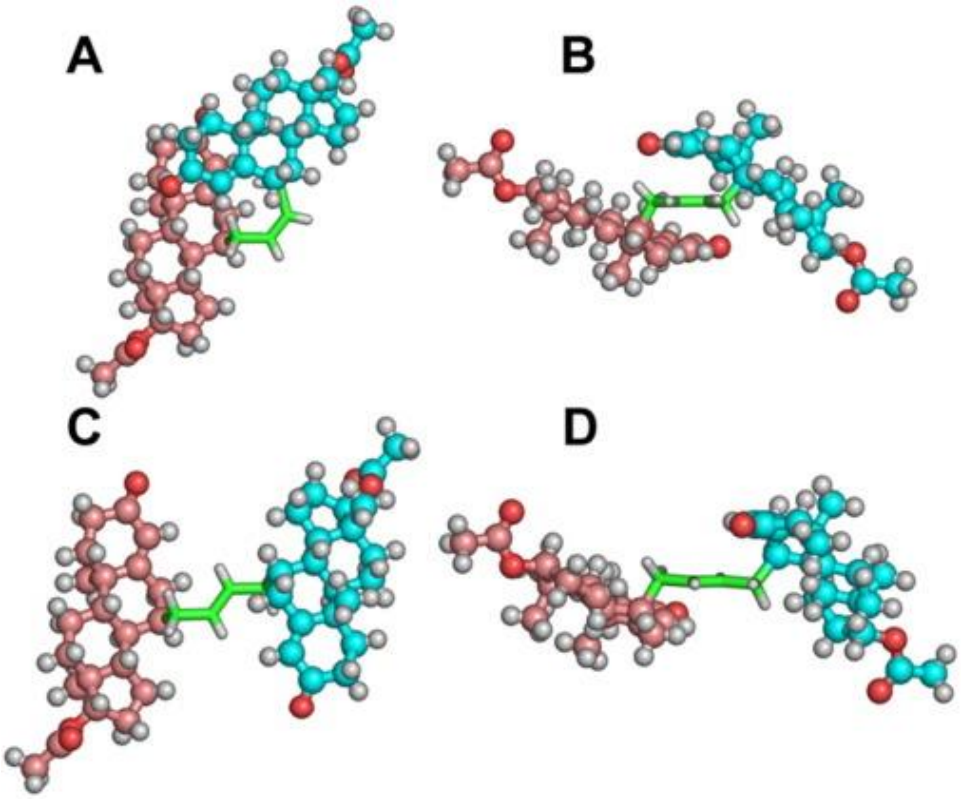

Fig. 1. The structures of TST dimers, *cis*-TST_2 (A, B) and *trans*-TST_2 (C, D) are shown: top view with steroid moiety in the plane of the figure (A, C) and side view (B, D). For *cis*-TST_2 the X-ray structure of diacetate dimer is shown as reported in,[18] while structure of *trans*-TST_2 is obtained from that of *cis* isomer by rotation around double bond connecting two TST monomers.

Journal of Inorganic Biochemistry, Vol 158, (May 2016): pg. 77-85. DOI. This article is © Elsevier and permission has been granted for this version to appear in e-Publications@Marquette. Elsevier does not grant permission for this article to be further copied/distributed or hosted elsewhere without the express permission from Elsevier.

***NOT THE PUBLISHED VERSION;* this is the author's final, peer-reviewed manuscript.** The published version may be accessed by following the link in the citation at the bottom of the page.

2. Experimental

2.1. Sample preparation

2.1.1. Materials

Testosterone dimers were synthesized as described earlier[18] from 7α-allyltestosterone acetate as a precursor. The latter was made using a three-step reaction sequence from testosterone. The dimerization step performed using Hoveyda–Grubbs' metathesis catalyst[22,23] yielded a mixture of *cis* and *trans* dimers diacetate (1:2 ratio). The *cis* and *trans* dimers diacetate were separated by flash column chromatography using distilled solvents (hexane/acetone, 4:1).[18] Once separated, thin layer chromatography showed a single homogeneous spot. Hydrolysis of the pure diacetate dimers were performed separately to yield the final *cis*-TST_2 and *trans*-TST_2 dimers. The final dimers remained homogeneous by thin layer chromatography. They were characterized by ^{1}H and ^{13}C NMR spectra and were exempt of any impurities. X-ray structure of the diacetate *cis*-TST_2 dimer confirmed the results of synthesis and separation, together with IR and NMR spectroscopy and mass-spectrometry.[18] All other chemicals of highest purity were from Sigma-Aldrich and used without further purification.

2.1.2. Protein expression and purification

Expression and purification of CYP3A4 and membrane scaffold protein (MSP1D1) and incorporation of CYP3A4 in POPC Nanodiscs was performed as described.[21,24] CYP3A4 with a C-terminal pentahistidine tag was expressed from the NF-14 construct in the PCWori + vector generously provided by Dr. F. P. Guengerich (Vanderbilt University, Nashville, TN). Assembly of CYP3A4 in Nanodiscs was done by gradual removal of detergent from the mixture of solubilized POPC lipids, CYP3A4 and MSP1D1 scaffold protein using Biobeads.[24]

Journal of Inorganic Biochemistry, Vol 158, (May 2016): pg. 77-85. DOI. This article is © Elsevier and permission has been granted for this version to appear in e-Publications@Marquette. Elsevier does not grant permission for this article to be further copied/distributed or hosted elsewhere without the express permission from Elsevier.

***NOT THE PUBLISHED VERSION;* this is the author's final, peer-reviewed manuscript.** The published version may be accessed by following the link in the citation at the bottom of the page.

2.2. Resonance Raman measurements

2.2.1. Preparation of samples for rR measurements

The samples of ~ 50 μM CYP3A4 in Nanodiscs were in 100 mM potasium phosphate buffer, pH 7.4. The TST, *cis*-TST_2 and *trans*-TST_2 bound samples contained 450 μM concentrations of TST, 63 μM of the *cis*-TST_2 and 75 μM of *trans*-TST_2, and the spin state conversion, estimated by electronic absorption spectrophotometry was 84%, 100% and 75% high spin, respectively. The carbonmonoxy ferrous ND:CYP3A4 samples were prepared as follows. The 100 μL of ~ 50 μM ferric ND:CYP3A4 sample was placed in a 5 mm NMR tube (WG-5 Economy, Wilmad), closed with a rubber septum and saturated with CO gas for ~ 30 min, while gently shaking in an ice bath. The sample was reduced by addition of ~ 2–4 M equivalents (~ 2–3 μL) of sodium dithionite dissolved in freshly degassed 100 mM potassium phosphate buffer, pH 7.4. The full conversion of ferric sample to ferrous CO adducts was monitored by UV–Vis, with no evidence being found for the presence of P420 before and after rR measurements, e.g., the ferrous CO P450 has a Soret at 448 nm and a Q-band at 552 nm, while Soret band of ferrous CO P420 is at 420 nm and Q-bands at around 540 nm and 570 nm.[25]

2.2.2. Acquisition of rR spectra

The resonance Raman spectra of ND:CYP3A4 samples were acquired using a Spex 1269 spectrometer equipped with a Spec-10 LN-cooled detector (Princeton Instruments, NJ). The ferric CYP3A4 samples were measured with the 406.7 nm excitation line from a Kr^+ laser (Coherent Innova Sabre Ion Laser) while the Fe(II)–CO adducts were excited using the 441.6 nm line provided by a He–Cd laser (IK Series He–Cd laser, Kimmon Koha CO., LTD.). The rR spectra were collected using back scattering (180°) geometry with the laser beam being focused by a cylindrical lens to form a line image on the sample.[26] The laser power was adjusted to ~ 10 mW, while for ferrous CO adducts it was kept at ~ 1 mW to minimize photodissociation. The slit width was set at 150 μm and the 1200 g/mm grating was used. Spectra were calibrated with fenchone (Sigma-Aldrich, WI), toluene-$^2H_6$ and acetone-$^2H_6$ (Cambridge Isotope Laboratories, Inc., MA) and

Journal of Inorganic Biochemistry, Vol 158, (May 2016): pg. 77-85. DOI. This article is © Elsevier and permission has been granted for this version to appear in e-Publications@Marquette. Elsevier does not grant permission for this article to be further copied/distributed or hosted elsewhere without the express permission from Elsevier.

***NOT THE PUBLISHED VERSION;* this is the author's final, peer-reviewed manuscript.** The published version may be accessed by following the link in the citation at the bottom of the page.

processed with Grams/32 AI software (Galactic Industries, Salem, NH). The peak fitting procedure was performed as previously published.[16]

2.3. Spectral titration studies

For the spectral titration studies the DMSO stock solutions of TST dimers have been used so that the final concentration of DMSO would not exceed 2%. UV–VIS spectral titrations have been done using Cary 3 spectrophotometer in the 10 mm quartz cells at the constant temperature 25 °C and ND:CYP3A4 concentration ~ 1 μM. Spectra were collected in the range 350–750 nm and analyzed using Singular Value Decomposition algorithm implemented in MATLAB as described earlier.[10] The second singular value corresponding to the difference spectrum was used for the fitting as a function of the substrate concentration with non-cooperative Langmuir equation or with Hill equation. Mixed titration experiments were done using the mixture of monomeric TST and *trans*-TST_2 at the constant 4:1 M ratio in order to probe the possible effect of monomeric TST binding to the CYP3A4 at the peripheral binding site as explained in Results and Discussion section.

3. Results and discussion

3.1. Resonance Raman studies

3.1.1. Ferric ND:CYP3A4

The high frequency rR spectrum of substrate-free ND:CYP3A4 is shown in Fig. 2 trace A. The dominant oxidation state marker band, ν_4 at 1372 cm^{-1}, indicates that the sample is in the ferric state and the spin state markers at 1502 cm^{-1} (ν_3), 1568 cm^{-1} (ν_2) and 1643 cm^{-1} (ν_{10}) are characteristic for low-spin (S = 1/2) state; it is noted, however, that the presence of a low intensity ν_3 mode at around 1488 cm^{-1} signals the presence of a small population of a high spin component. The percentage of high spin component in this sample was calculated according to previously reported procedure[27] and was estimated to be 15%, in good agreement with the value obtained from UV–Vis spectrophotometry and previously published results.[16]

Journal of Inorganic Biochemistry, Vol 158, (May 2016): pg. 77-85. DOI. This article is © Elsevier and permission has been granted for this version to appear in e-Publications@Marquette. Elsevier does not grant permission for this article to be further copied/distributed or hosted elsewhere without the express permission from Elsevier.

***NOT THE PUBLISHED VERSION;* this is the author's final, peer-reviewed manuscript.** The published version may be accessed by following the link in the citation at the bottom of the page.

The spectral peaks associated with vinyl stretching modes are seen at 1625 cm^{-1} and 1636 cm^{-1}. Addition of a saturating amount of monomeric TST substrate (trace B) resulted in substantial spin state conversion to high spin (calculated 74% HS from rR data and 84% from electronic absorption spectrophotometric data) as is manifested the clear appearance of the high spin state marker modes; namely, the ν_3 mode at 1488 cm^{-1} and the ν_2 at 1570 cm^{-1}. The ν_{10} high spin mode expected near 1625 cm^{-1} is buried in envelope containing the $\nu(C{=}C)$ stretching modes. These results are consistent with previously published data.[16]

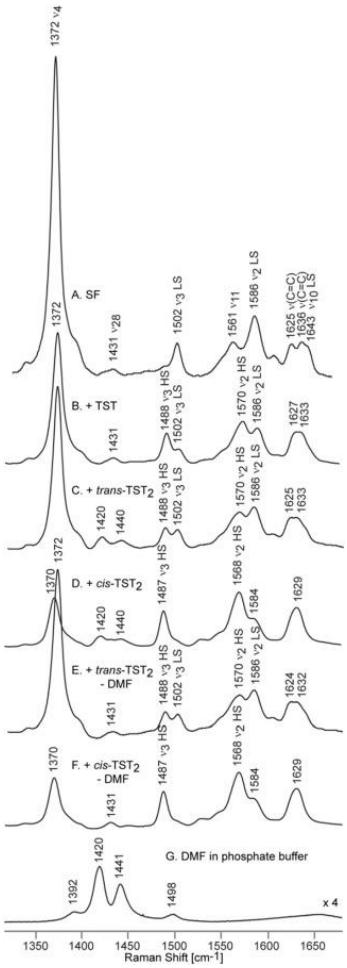

Fig. 2. The high frequency rR spectra of ferric ND-CYP3A4 samples in their substrate-free form (A), bound with excess of monomeric TST (B), *trans*-TST_2-bound (C), *cis*-TST_2-bound (D), *trans*-TST_2-bound minus DMF (E), *cis*-TST_2-bound minus DMF (F) and DMF in phosphate buffer (G). Excitation line 406.7 nm, spectra normalized to the ν_3 modes.

Journal of Inorganic Biochemistry, Vol 158, (May 2016): pg. 77-85. DOI. This article is © Elsevier and permission has been granted for this version to appear in e-Publications@Marquette. Elsevier does not grant permission for this article to be further copied/distributed or hosted elsewhere without the express permission from Elsevier.

***NOT THE PUBLISHED VERSION;* this is the author's final, peer-reviewed manuscript.** The published version may be accessed by following the link in the citation at the bottom of the page.

The spectra of *trans*-TST_2 (trace C) and *cis*-TST_2 (trace D) bound samples contain modes associated with DMF that was used as a solvent for the stock solutions of these substrates (trace G). The most intense modes associated with the DMF solvent are observed at 1420 cm^{-1} and 1441 cm^{-1}. In order to avoid complication that might arise from overlap of CYP3A4 modes with these solvent bands, the spectrum of DMF was subtracted from the spectra of TST-dimer bound samples, with the resultant spectra being presented in trace E for *trans*-TST_2 and trace F for *cis*-TST_2 samples, respectively. As can be clearly seen, *trans*-TST_2 causes only partial spin state conversion upon binding (calculated 49% HS), *cis*-TST_2 forces almost complete spin state conversion (calculated 92% HS).

The corresponding spectra in the low frequency region are presented in Fig. 3, the left panel presenting CYP3A4 spectra was normalized to the ν_8 mode for a better view of small intensity modes, while the right panel was normalized to the intense ν_7 mode at 674 cm^{-1}. As was the case in the high frequency region, the samples containing *cis*-TST and *trans*-TST contain dimethylformamide (DMF) (traces C and D), with the DMF bands being subtracted to yield traces E and F. The relative intensity ratios of Raman modes of DMF solvent shown at the bottom of left and right panels have not been altered when splitting the full spectrum. The ferric substrate-free (SF) (trace A) and TST (trace B) samples exhibit similar spectral pattern to that observed previously;[13] e.g., the spectrum of TST-bound sample exhibits significantly enhanced out-of-plane (OOP) modes at 317 cm^{-1} and 499 cm^{-1} as compared to the spectrum of substrate-free form. The spectrum of the TST-bound sample (trace B) contains slightly enhanced OOP modes as compared to the spectrum of the *trans*-TST_2-bound sample (trace E). This slight alteration reflects smaller percentage of high spin population in the *trans*-TST_2-bound and is consistent with observations in the high frequency region. On the other hand, the low frequency rR spectrum of the ferric *cis*-TST_2-bound sample exhibits relatively strong enhancement of OOP modes, stronger enhancement of in-plane vinyl mode at 411 cm^{-1} that is accompanied by the upshift of the propionate bending mode by 2 cm^{-1} and the activation of a $\delta(C_\beta\text{-}C)$ bending mode, ν_{51}, appearing at 327 cm^{-1}, which might be associated with another propionate bending motion.

Journal of Inorganic Biochemistry, Vol 158, (May 2016): pg. 77-85. DOI. This article is © Elsevier and permission has been granted for this version to appear in e-Publications@Marquette. Elsevier does not grant permission for this article to be further copied/distributed or hosted elsewhere without the express permission from Elsevier.

***NOT THE PUBLISHED VERSION;* this is the author's final, peer-reviewed manuscript.** The published version may be accessed by following the link in the citation at the bottom of the page.

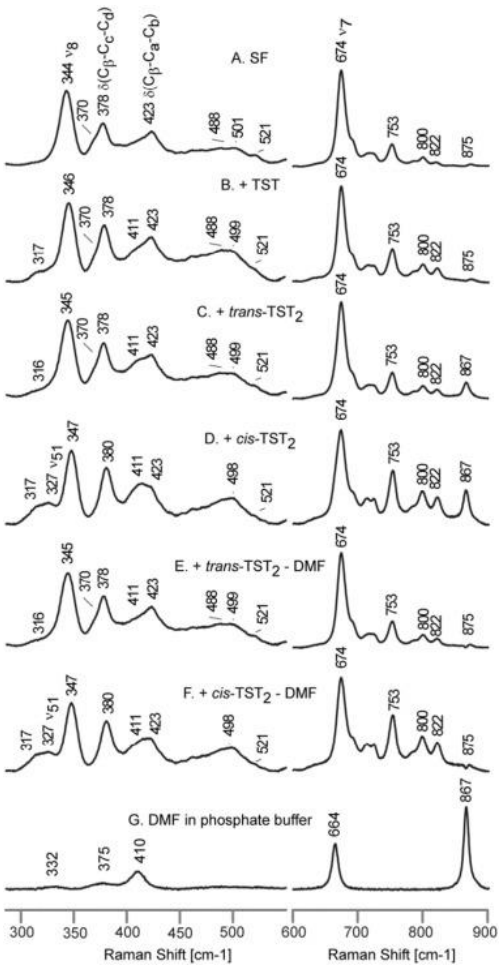

Fig. 3. The low frequency rR spectra of ferric ND:CYP3A4 samples in their substrate-free form (A), bound with excess of monomeric TST (B), *trans*-TST_2-bound (C), *cis*-TST_2-bound (D), *trans*-TST_2-bound minus DMF (E), *cis*-TST_2-bound minus DMF (F) and DMF in phosphate buffer (G), excitation line 406.7 nm. The left panel of CYP3A4 spectra is normalized to the v_8 modes for a better view of small modes, while the right panel is normalized to the v_7 mode. The relative intensities of the Raman bands in the spectrum of DMF in buffer are unchanged.

Collectively, the binding of *trans*-TST_2 substrate to the ferric protein causes similar spectral changes to those seen when binding of monomeric TST molecules, with slightly smaller spin state conversion. Conversely, binding of *cis*-TST_2 substrate causes large spin state conversion (92% HS by rR measurement), significant changes in heme planarity and changes in the disposition of heme peripheral groups. These observations imply that the *trans*-TST_2 substrate binds in a similar manner as a pair of the monomeric TSTs, while the *cis*-TST_2 dimer occupies significantly different position than do two TST monomers.

Journal of Inorganic Biochemistry, Vol 158, (May 2016): pg. 77-85. DOI. This article is © Elsevier and permission has been granted for this version to appear in e-Publications@Marquette. Elsevier does not grant permission for this article to be further copied/distributed or hosted elsewhere without the express permission from Elsevier.

***NOT THE PUBLISHED VERSION;* this is the author's final, peer-reviewed manuscript.** The published version may be accessed by following the link in the citation at the bottom of the page.

3.1.2. Ferrous CO adducts of ND:CYP3A4

The v(Fe–C) stretching modes of SF and TST-bound ND:CYP3A4 are observed as wide, asymmetrical envelopes, with components at 476 cm^{-1} and 491 cm^{-1}, respectively (Fig. 4). Generally, these spectra can be deconvoluted into two Fe–C modes, centered at 476 cm^{-1} and 491 cm^{-1}, with the lower frequency one being dominant in the spectrum of SF sample and the higher frequency one being dominant for TST-bound sample, in agreement with previously published data.[16] The corresponding two CO stretching modes are seen at 1953 cm^{-1} and 1929 cm^{-1}, respectively, and are observed in spectra of both SF and TST-bound samples, but with reversed intensities (Fig. 5). There are no significant changes in heme mode disposition upon binding of the TST molecules (Fig. 4 and Fig. 5). The ferrous ion of CO adduct is in a six coordinate, low-spin state, as seen by the positions of the oxidation state marker (v_4), at 1370 cm^{-1}, and the spin state marker band (v_3), at 1496 cm^{-1}, data consistent with those previously published (Fig. 5).[16]

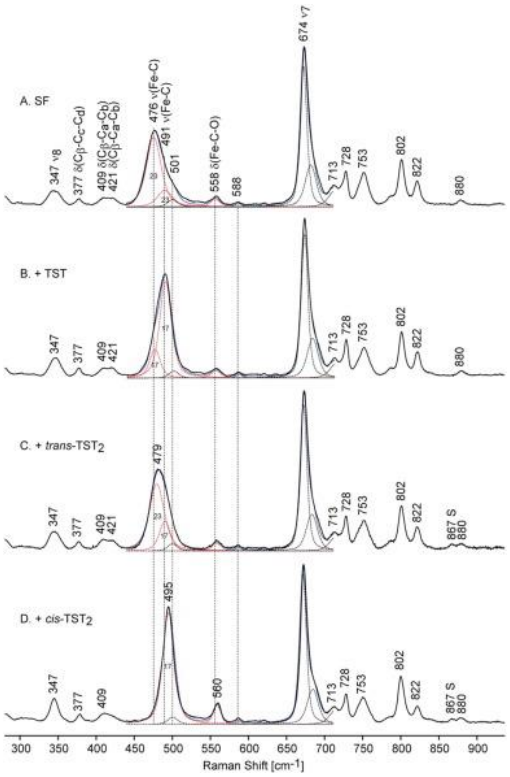

Fig. 4. The low frequency rR spectra of ferrous CO adducts of ND:CYP3A4 samples in theirsubstrate-free form (A), bound with excess of monomeric TST (B), trans-TST2-

***NOT THE PUBLISHED VERSION;* this is the author's final, peer-reviewed manuscript.** The published version may be accessed by following the link in the citation at the bottom of the page.

bound (C) and cis-TST2-bound (D). Excitation line 441.6 nm, the spectra were normalized to the v7 mode. The Fe–C bands in the 450–700 cm−1 region were deconvoluted using 50% Gaussian and 50% Lorentzian functions as described before.[16] Black solid line — experimental data, blue solid line — fitted spectra, red dotted line — modes associated with v(Fe–C) modes, black dotted line — other modes in this region. The horizontal numbers indicate the bandwidths of the v(Fe–C) modes reflecting the effects of the substrate binding on the Fe–C–O fragment.

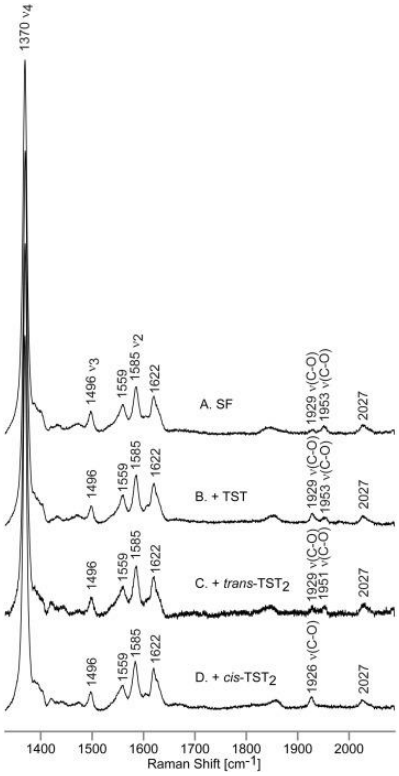

Fig. 5. The high frequency rR spectra of ferrous CO adducts of ND:CYP3A4 samples in their substrate-free form (A), bound with excess of monomeric TST (B), *trans*-TST_2-bound (C) and *cis*-TST_2-bound (D). Excitation line 441.6 nm, the spectra were normalized to the v_4 mode.

The spectrum of CO bound ferrous *trans*-TST_2 sample exhibits a wide v(Fe–CO) envelope cantered at around 483 cm^{-1}, which can be reasonably deconvoluted in the same way as the previously discussed spectra of SF and TST-bound samples. However, the lower frequency Fe–C stretching mode is upshifted to 479 cm^{-1} (with it corresponding v(C–O) mode accordingly shifting down by 2 cm^{-1}); the higher frequency one is observed at 491 cm^{-1}, with its v(C–O) at 1929 cm^{-1} also unshifting. The δ(Fe–C–O) bending modes for all three samples, SF, TST-bound and *trans*-TST_2-bound are observed at around 558 cm^{-1}.

***NOT THE PUBLISHED VERSION;* this is the author's final, peer-reviewed manuscript.** The published version may be accessed by following the link in the citation at the bottom of the page.

The unique spectrum of the *cis*-TST_2-bound sample exhibits only one, very intense and sharp, ν(Fe–C) stretching mode at 495 cm^{-1}; this mode is accompanied by strong δ(Fe–C–O) bending mode seen at 560 cm^{-1} and a ν(CO) stretching mode at 1926 cm^{-1} (Fig. 5). More careful analysis of the 450–700 cm^{-1} regions reveals that the peak area ratios of δ(Fe–C–O) bending mode to the ν_7 mode is 1:28 for SF sample, 1:31 for TST-bound sample, 1:32 for *trans*-TST_2 and 1:11 for *cis*-TST_2. The approximately three times larger intensity of δ(Fe–C–O) bending mode in *cis*-TST2 sample implies unusually large bending of the Fe–C–O conformer.[28] The additional strong intensity of the ν(Fe–C) and its narrow bandwidth indicate also very rigid conformational restriction of the Fe–C–O fragment imposed by the presence of *cis*-TST_2 substrate. It is noted that the only significant changes in heme modes upon binding all three substrates to the ferrous CO adducts is the slight decrease in intensity of the higher frequency bending mode (at 421 cm^{-1}) of the *cis*-TST_2 dimer. Thus, the rR data of ferric and ferrous CO adducts of the *trans*-TST_2- and *cis*-TST_2-bound samples, although reflecting isolated states with only two TST molecules, are very different from each other. The *trans*-TST_2 substrate causes changes in the spectra of ferric and ferrous CO states similar to those observed using excess of monomeric TST, therefore representing the state more similar to the natural situation with two monomeric TST bound. On the other hand, binding of the *cis*-TST_2 substrate in the ferric state causes unusually strong spin shift. It also causes relatively strong heme deformation as seen by increase in intensity of the OOP modes as well as changes in the heme peripheral groups (Fig. 3, trace F). Moreover, the rR spectra of ferrous CO adduct show that the *cis*-TST_2 substrate, although generally not affecting the heme modes in this ligated state, does cause strong deformation of the Fe–C–O fragment, indication of different occupation of heme pocket as compared to the monomeric TST and the *trans*-TST_2 dimer.

3.2. Spectral binding studies

Titration of CYP3A4 with *trans*-TST_2 and *cis*-TST_2 were studied using absorption spectroscopy. As shown in Fig. 6, binding of *cis*-TST_2 is very tight, with K_d = 0.3 μM and almost complete conversion from predominantly low-spin to the high spin state (Fig. 6, A and B). For the *trans*-TST_2 dimer binding is 25-fold weaker, with K_d = 8 μM and spin

***NOT THE PUBLISHED VERSION;* this is the author's final, peer-reviewed manuscript.** The published version may be accessed by following the link in the citation at the bottom of the page.

shift at maximum ~ 75% (Fig. 6, C and D). Therefore, interactions of ND:CYP3A4 with *cis*-TST_2 and *trans*-TST_2 show significant variations in both affinity and the amplitude of the spin shift, indicating substantially different binding modes. Both dimers have identical chemical structure, but significant difference in their shapes results in the large difference in their affinities. Very tight binding of *cis*-TST_2 and ~ 100% high spin conversion suggest close packing of this TST dimer in the immediate vicinity of the heme with complete displacement of water as the sixth ligand to the iron. Binding of the *trans*-TST_2 dimer results in a looser fit in the active site, as judged by incomplete spin shift reached at saturation. The inability of *trans*-TST_2 to completely displace the water molecule ligating to the heme iron suggests more dynamic positioning of this TST dimer inside the substrate binding pocket and possible existence of multiple conformers with different distances of steroid moiety from the heme. This suggestion is strongly supported by the rR data observed for these two cases, where the *trans*-TST_2 dimer exhibits two ν(Fe–C) and two ν(C–O) modes as opposed to the single (sharp) modes observed for the *cis*-TST_2 dimer. This loose binding and easier access of water to the substrate binding pocket may explain, at least in part, the ~ 25-fold lower affinity of CYP3A4 for the *trans*-TST_2 than that observed for *cis*-TST_2. Although for *trans*-TST_2 dimer binding is substantially weaker than for *cis*-TST_2, it is still more tight than with monomeric TST (K_d = 19 μM and 37 μM for the first and second binding event with TST monomer, (10)). The higher affinity of both TST dimers to CYP3A4 underlines important contribution of hydrophobic interactions of lipophilic substrates with xenobiotic metabolizing cytochromes P450.[29]

Journal of Inorganic Biochemistry, Vol 158, (May 2016): pg. 77-85. DOI. This article is © Elsevier and permission has been granted for this version to appear in e-Publications@Marquette. Elsevier does not grant permission for this article to be further copied/distributed or hosted elsewhere without the express permission from Elsevier.

***NOT THE PUBLISHED VERSION;* this is the author's final, peer-reviewed manuscript.** The published version may be accessed by following the link in the citation at the bottom of the page.

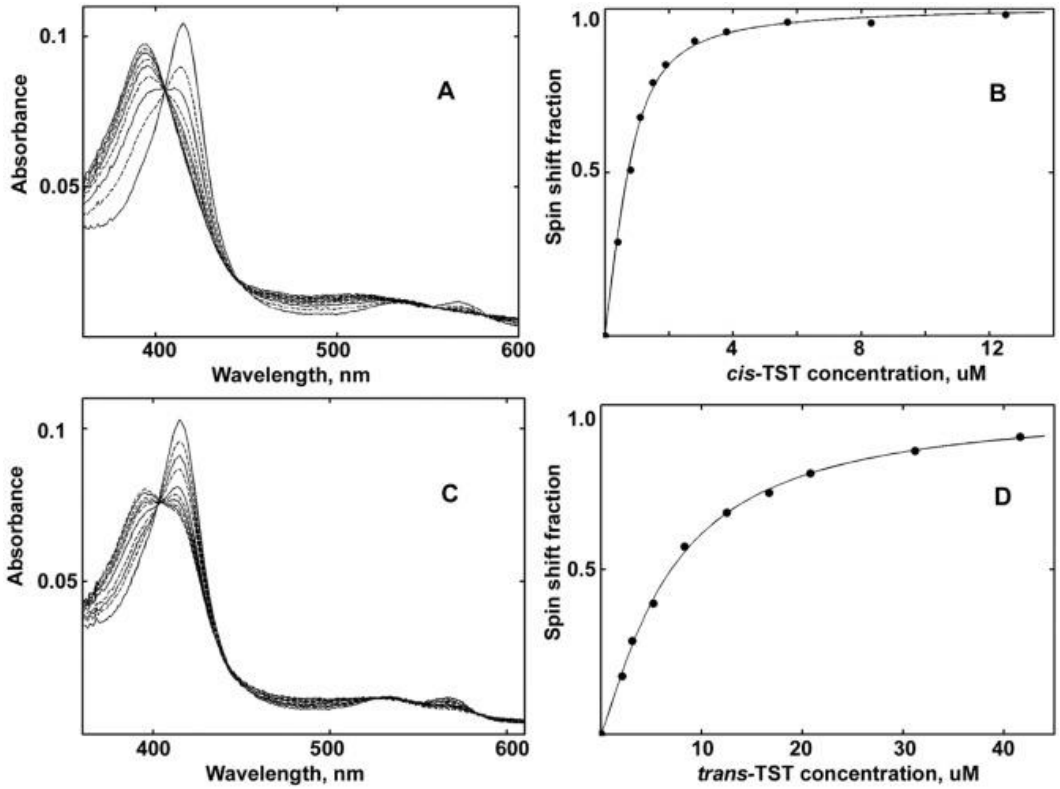

Fig. 6. Titration of ND:CYP3A4 with *cis*-TST_2 (top) and *trans*-TST_2 (bottom). Experimental results (filled circles) shown as fractions of total spin shift as a function of substrate concentration have been fitted with the regular Langmuir binding isotherm calculated using exact solution for the tight binding case (top), or Hill equation for the cooperative binding (bottom).

Because of the large size of both TST dimers, simultaneous incorporation of two such molecules into the active site of CYP3A4 is highly disfavored. As expected, no apparent cooperativity is seen in the spectral titration curves shown in Figs. 6B and D. The fit of the data shown in Fig. 6D is slightly better when Hill equation is used (n_H = 1.2), although low value of the Hill coefficient also confirms non-cooperative binding in CYP3A4.[6] Minor deviations from the Langmuir isotherm may be attributed to partitioning of the *trans*-TST_2 into the lipid bilayer of POPC Nanodiscs, although the effect of such partitioning is small at low concentration of Nanodiscs (1 μM ND:CYP3A4 concentration used in titration experiments corresponds to ~ 10^{-4} volume fraction of lipid phase in solution). While the possibility of interaction of the *trans*-TST_2 with peripheral site of CYP3A4 cannot be ruled out, results of titration experiments with both TST dimers suggest the simple single-site binding and do not indicate any multisite cooperative interactions.

Journal of Inorganic Biochemistry, Vol 158, (May 2016): pg. 77-85. DOI. This article is © Elsevier and permission has been granted for this version to appear in e-Publications@Marquette. Elsevier does not grant permission for this article to be further copied/distributed or hosted elsewhere without the express permission from Elsevier.

***NOT THE PUBLISHED VERSION;* this is the author's final, peer-reviewed manuscript.** The published version may be accessed by following the link in the citation at the bottom of the page.

In order to explore the possible effect of binding at the peripheral allosteric site we performed titration of CYP3A4 with the mixture of monomeric TST with *trans*-TST_2, assuming that monomeric TST will be able to bind to the peripheral site with no competition from TST dimer. Such combination of two substrates, of which one can bind to the allosteric site with relatively high affinity[10] while the other one does not, provides an excellent opportunity for evaluating the allosteric effect of TST monomer at the peripheral site on the binding of TST dimer inside the substrate binding pocket.

Titration with the mixture of monomeric TST with *trans*-TST_2 (4:1 ratio) results in ~ 2-fold higher apparent affinity with the K_d decreasing from 8 μM to 3.4 μM. In addition, a significant shift of the spin equilibrium towards high spin configuration is observed at saturation, changing the remaining LS fraction from 25% to ~ 4%. This effect of TST monomer can be attributed to binding at the remote allosteric site[15] rather than to insertion into the active site in addition to the bound *trans*-TST_2, which is unlikely for steric reasons. Competitive replacement of the *trans*-TST_2 by two monomeric TST molecules can also be ruled out because of low TST concentration in the mixed titration experiment. From earlier studies performed under similar conditions[10,30] it is known that high spin conversion in CYP3A4 in Nanodiscs can be reached only at TST concentrations ~ 200 μM, i.e. much higher than the maximum 75 μM concentrations reached in this study (Fig. 7, mixed titration). Thus, binding of monomeric TST in the active site would require significant increase of CYP3A4 affinity to this substrate in the presence of *trans*-TST_2, for which we have no experimental evidence. Therefore, our observations provide a direct evidence of the functionally important allosteric effect caused by TST monomer binding at the remote site when another substrate is present in the substrate binding pocket. Similar effects have been observed in the mixed titration of CYP3A4 with carbamazepine and various steroids,[15] in which apparent positive cooperativity was detected by the shift of the midpoint of the spin shift transition towards the lower concentrations of substrates. Taken together, these experimental results suggest the presence of the general regulatory role of steroids upon CYP3A4 catalysis (at least with some substrates) via binding at the remote allosteric site formed at the interface between F-F' and G-G' loops of the protein and lipid head groups.

Journal of Inorganic Biochemistry, Vol 158, (May 2016): pg. 77-85. DOI. This article is © Elsevier and permission has been granted for this version to appear in e-Publications@Marquette. Elsevier does not grant permission for this article to be further copied/distributed or hosted elsewhere without the express permission from Elsevier.

***NOT THE PUBLISHED VERSION;* this is the author's final, peer-reviewed manuscript.** The published version may be accessed by following the link in the citation at the bottom of the page.

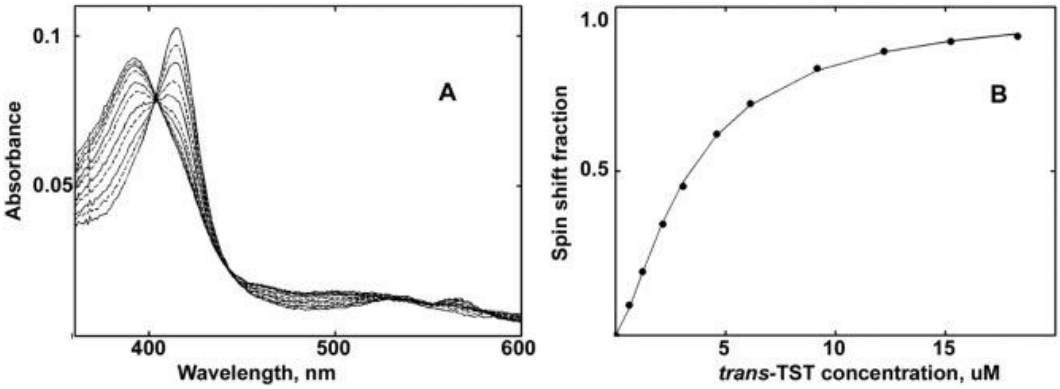

Fig. 7. Titration of ND:CYP3A4 with the mixture of *trans*-TST_2 and monomeric TST at 1:4 ratio.

4. Discussion

Currently, there is no X-ray structure of CYP3A4 with steroid substrates bound in the substrate binding pocket, the only ones, having a progesterone bound,[13,14] have it located at the peripheral non-productive site. Several structures of other cytochromes P450, which have one steroid substrate molecule in a productive position, including CYP154C5,[31] CYP7A1,[32] CYP11A1,[33,34] CYP11B2,[35] CYP19A1,[36] human CYP17A1,[37] fish CYP17A1 and CYP17A2,[38] CYP46A1,[39] CYP51[40] and CYP125,[41] demonstrate various orientations of the steroid moiety with respect to the heme iron and I-helix, the main structural elements shaping the P450 active site. However, the presence of the second steroid in the active site is expected to impose significant restrictions on the stereochemistry of packing of two substrate molecules within the substrate binding cavity. This can be seen in the only two X-ray structures of cytochromes P450 with two steroid molecules bound inside the active site, P450eryF with two androstenedione molecules,[42] and CYP21A2 with two 17OH-progesterone molecules.[43] In the former case two steroids are packed one over another, almost parallel to the I-helix, while in the latter the second steroid is significantly shifted with respect to the first one. In the present work, the synthetic TST dimers with *cis*- and *trans*-configurations allowed us to compare these two binding modes for two TST monomers to CYP3A4 in a straightforward manner.

Our results show that both *cis*-TST_2 and *trans*-TST_2 can bind to the CYP3A4, which possesses highly flexible active site capable to accommodate such different substrates. However, *cis*-TST_2 binds much

Journal of Inorganic Biochemistry, Vol 158, (May 2016): pg. 77-85. DOI. This article is © Elsevier and permission has been granted for this version to appear in e-Publications@Marquette. Elsevier does not grant permission for this article to be further copied/distributed or hosted elsewhere without the express permission from Elsevier.

***NOT THE PUBLISHED VERSION;* this is the author's final, peer-reviewed manuscript.** The published version may be accessed by following the link in the citation at the bottom of the page.

more tightly and induces ~ 100% spin shift, presumably due to more compact shape and better fit to the substrate binding pocket as compared to *trans*-TST_2. One the other hand, it is important to emphasize that the *trans*-TST_2 dimer exhibits spectral (rR) properties and binding affinity more closely matching those extracted for the case with two monomeric TST substrates. This is in agreement with its more flexible and somewhat larger shape in comparison to the *cis*-TST_2 dimer (see Fig. 1) that allows comparable binding interactions to the CYP3A4 as do two TSTs.

Comparison with rR studies of other cytochromes P450 reveals a variety of observed spectral changes and corresponding structural perturbations caused by substrate binding. No distinct changes in the heme modes were observed in the human CYP17A1 upon binding of the natural substrates progesterone and others, despite almost 100% spin shift caused by progesterone binding.[44] Similarly, no perturbation of the heme modes were detected upon substrate binding to CYP2B4.[45] However, in CYP101 significant perturbation of the low frequency heme modes caused by substrate binding were observed[46,47] and attributed to substantial out-of-plane movements of the vinyl side chains and perturbations of the propionate side chains. Similar perturbations were observed also in CYP51 from *Mycobacterium Tuberculosis* upon binding of azole inhibitors[48] and substrate dihydrolanosterol;[49] such changes were also seen in human prostacycline synthase in the presence of some substrate analogs, but not inhibitors.[50]

Interestingly, there are other examples of stronger binding of dimers of substrates to CYP3A4. Synthetic dimers of furanocoumarins proved to be very strong inhibitors of TST hydroxylation by CYP3A4.[51,52] Several natural polyphenols, such as ε-viniferin, the dimer of resveratrol,[53] and rivulobirin-A, a natural furanocoumarin dimer,[54] also appear to be potent inhibitors of CYP3A4. These results are consistent with the general approach for using synthetic dimers of CYP3A4 substrates or inhibitors to improve binding.

In conclusion, our results directly demonstrate the ability of CYP3A4 to accommodate two TST molecules inside the substrate binding pocket in various configurations. The degree of spin shift and binding affinity strongly depend on the geometry and overall size of

Journal of Inorganic Biochemistry, Vol 158, (May 2016): pg. 77-85. DOI. This article is © Elsevier and permission has been granted for this version to appear in e-Publications@Marquette. Elsevier does not grant permission for this article to be further copied/distributed or hosted elsewhere without the express permission from Elsevier.

***NOT THE PUBLISHED VERSION;* this is the author's final, peer-reviewed manuscript.** The published version may be accessed by following the link in the citation at the bottom of the page.

TST dimers. In addition, interaction of TST monomer with CYP3A4 at the remote site of the enzyme significantly increases spin shift and binding affinity for the *trans*-TST_2. This observation confirms earlier suggestions on the possible allosteric effect caused by binding of steroids at the allosteric site,[7,10,19,20,21] tentatively the one identified as the progesterone binding site by X-ray crystallography[13]

Table of Abbreviations

DMF dimethylformamide
HS high-spin fraction
LS low-spin fraction
ND:CYP3A4 Nanodiscs with CYP3A4
POPC 1-palmitoyl-2-oleoyl-sn-glycero-3-phosphocholine
rR resonance Raman
SF substrate free
TST testosterone
cis-TST_2 *cis*-testosterone dimer
trans-TST_2 *trans*-testosterone dimer

Acknowledgments

This work was supported by National Institutes of Health grants GM33775 to S. G. S., GM96117 to J. R. K, and GM110428 to S. G. S. and J. R. K. The authors wish to thank the Fonds de Recherche du Québec-Nature et Technologies (FRQNT) for financial support (Grant 132839).

References

[1] Guengerich, F. P. (2014) Experimental approaches to analysis of reactions of cytochrome P450 enzymes, In *Drug Metabolism Prediction* (Kirchmair, J., Ed.), pp 199–219, Wiley-VCH Verlag, Weinheim, Germany.

[2] F.P. Guengerich. Human cytochrome P450 enzymes. P.R. Ortiz de Montellano (Ed.), Cytochrome P450. *Structure, Mechanism, and Biochemistry* (fourth ed.), Springer, Heidelberg (2015), pp. 523–786

[3] R.S. Foti, L.C. Wienkers, J.L. Wahlstrom. Application of cytochrome P450 drug interaction screening in drug discovery. *Comb. Chem. High Throughput Screen*., 13 (2010), pp. 145–158

[4] W.M. Atkins. Current views on the fundamental mechanisms of cytochrome P450 allosterism. *Expert Opin. Drug Metab. Toxicol*., 2 (2006), pp. 573–579

***NOT THE PUBLISHED VERSION;* this is the author's final, peer-reviewed manuscript.** The published version may be accessed by following the link in the citation at the bottom of the page.

[5] A. Boobis, J.B. Watelet, R. Whomsley, M.S. Benedetti, P. Demoly, K. Tipton. Drug interactions. *Drug Metab. Rev*., 41 (2009), pp. 486–527

[6] I.G. Denisov, D.J. Frank, S.G. Sligar. Cooperative properties of cytochromes P450. *Pharmacol. Ther*., 124 (2009), pp. 151–167

[7] I.G. Denisov, S.G. Sligar. A novel type of allosteric regulation: functional cooperativity in monomeric proteins. *Arch. Biochem. Biophys.*, 519 (2012), pp. 91–102

[8] R.S. Obach, R.L. Walsky, K. Venkatakrishnan, E.A. Gaman, J.B. Houston, L.M. Tremaine. The utility of in vitro cytochrome P450 inhibition data in the prediction of drug-drug interactions. *J. Pharmacol. Exp. Ther.*, 316 (2006), pp. 336–348

[9] I.F. Sevrioukova, T.L. Poulos. Understanding the mechanism of cytochrome P450 3A4: recent advances and remaining problems. *Dalton Trans*., 42 (2013), pp. 3116–3126

[10] I.G. Denisov, B.J. Baas, Y.V. Grinkova, S.G. Sligar. Cooperativity in cytochrome P450 3A4: linkages in substrate binding, spin state, uncoupling, and product formation. *J. Biol. Chem*., 282 (2007), pp. 7066–7076

[11] I.F. Sevrioukova, T.L. Poulos. Dissecting cytochrome P450 3A4-ligand interactions using ritonavir analogues. *Biochemistry*, 52 (2013), pp. 4474–4481

[12] M. Ekroos, T. Sjoegren. Structural basis for ligand promiscuity in cytochrome P 450 3A4. *Proc. Natl. Acad. Sci. U. S. A.,* 103 (2006), pp. 13682–13687

[13] P.A. Williams, J. Cosme, D.M. Vinkovic, A. Ward, H.C. Angove, P.J. Day, C. Vonrhein, I.J. Tickle, H. Jhoti. Crystal structures of human cytochrome P450 3A4 bound to metyrapone and progesterone. *Science*, 305 (2004), pp. 683–686

[14] I.F. Sevrioukova, T.L. Poulos. Anion-dependent stimulation of CYP3A4 monooxygenase. *Biochemistry*, 54 (2015), pp. 4083–4096

[15] I.G. Denisov, Y.V. Grinkova, J.L. Baylon, E. Tajkhorshid, S.G. Sligar. Mechanism of drug-drug interactions mediated by human cytochrome P450 CYP3A4 monomer. *Biochemistry*, 54 (2015), pp. 2227–2239

[16] P.J. Mak, I.G. Denisov, Y.V. Grinkova, S.G. Sligar, J.R. Kincaid. Defining CYP3A4 structural responses to substrate binding. Raman spectroscopic studies of a nanodisc-incorporated mammalian cytochrome P450. *J. Am. Chem. Soc*., 133 (2011), pp. 1357–1366

[17] I.F. Sevrioukova, T.L. Poulos. Structural and mechanistic insights into the interaction of cytochrome P4503A4 with bromoergocryptine, a type I ligand. *J. Biol. Chem*., 287 (2012), pp. 3510–3517

[18] D. Bastien, V. Leblanc, E. Asselin, G. Berube. First synthesis of separable isomeric testosterone dimers showing differential activities on prostate cancer cells. *Bioorg. Med. Chem. Lett.,* 20 (2010), pp. 2078–2081

***NOT THE PUBLISHED VERSION;* this is the author's final, peer-reviewed manuscript.** The published version may be accessed by following the link in the citation at the bottom of the page.

[19] D.R. Davydov, N.Y. Davydova, E.V. Sineva, I. Kufareva, J.R. Halpert. Pivotal role of P450–P450 interactions in CYP3A4 allostery: the case of alpha-naphthoflavone. *Biochem. J.,* 453 (2013), pp. 219–230

[20] D.R. Davydov, J.R. Halpert. Allosteric P450 mechanisms: multiple binding sites, multiple conformers or both? *Expert Opin. Drug Metab. Toxicol.*, 4 (2008), pp. 1523–1535

[21] I.G. Denisov, Y.V. Grinkova, M.A. McLean, S.G. Sligar. The one-electron autoxidation of human cytochrome P450 3A4. *J. Biol. Chem.,* 282 (2007), pp. 26865–26873

[22] T.M. Trnka, R.H. Grubbs. The development of L2X2Ru = CHR olefin metathesis catalysts: an organometallic success story. *Acc. Chem. Res.,* 34 (2001), pp. 18–29

[23] N.K. Yee, V. Farina, I.N. Houpis, N. Haddad, R.P. Frutos, F. Gallou, X.J. Wang, X. Wei, R.D. Simpson, X. Feng, V. Fuchs, Y. Xu, J. Tan, L. Zhang, J. Xu, L.L. Smith-Keenan, J. Vitous, M.D. Ridges, E.M. Spinelli, M. Johnson, K. Donsbach, T. Nicola, M. Brenner, E. Winter, P. Kreye, W. Samstag. Efficient large-scale synthesis of BILN 2061, a potent HCV protease inhibitor, by a convergent approach based on ring-closing metathesis. *J. Org. Chem*., 71 (2006), pp. 7133–7145

[24] I.G. Denisov, Y.V. Grinkova, B.J. Baas, S.G. Sligar. The ferrous-dioxygen intermediate in human cytochrome P450 3A4: substrate dependence of formation of decay kinetics. *J. Biol. Chem.,* 281 (2006), pp. 23313–23318

[25] S.A. Martinis, S.R. Blanke, L.P. Hager, S.G. Sligar, G.H. Hoa, J.J. Rux, J.H. Dawson. Probing the heme iron coordination structure of pressure-induced cytochrome P420cam. *Biochemistry*, 35 (1996), pp. 14530–14536

[26] D.F. Shriver, J.B.R. Dunn. The backscattering geometry for raman spectroscopy of colored materials. *Appl. Spectrosc*., 28 (1974), pp. 319–323

[27] P.J. Mak, Q. Zhu, J.R. Kincaid. Using resonance raman cross-section data to estimate the spin state populations of cytochromes P450. *J. Raman Spectrosc*., 44 (2013), pp. 1792–1794

[28] T.G. Spiro, A.V. Soldatova, G. Balakrishnan. CO, NO, and O_2 as vibrational probes of heme protein interactions. *Coord. Chem. Rev.,* 257 (2013), pp. 511–527

[29] T.L. Poulos, E.F. Johnson. Structures of cytochrome P450 enzymes. P.R. Ortiz de Montellano (Ed.), *Cytochrome P450: Structure, Mechanism, and Biochemistry* (fourth ed.), Springer, Heidelberg (2015), pp. 3–32

[30] B.J. Baas, I.G. Denisov, S.G. Sligar. Homotropic cooperativity of monomeric cytochrome P450 3A4 in a nanoscale native bilayer environment. *Arch. Biochem. Biophys*., 430 (2004), pp. 218–228

Journal of Inorganic Biochemistry, Vol 158, (May 2016): pg. 77-85. DOI. This article is © Elsevier and permission has been granted for this version to appear in e-Publications@Marquette. Elsevier does not grant permission for this article to be further copied/distributed or hosted elsewhere without the express permission from Elsevier.

***NOT THE PUBLISHED VERSION;* this is the author's final, peer-reviewed manuscript.** The published version may be accessed by following the link in the citation at the bottom of the page.

[31] K. Herzog, P. Bracco, A. Onoda, T. Hayashi, K. Hoffmann, A. Schallmey. Enzyme-substrate complex structures of CYP154C5 shed light on its mode of highly selective steroid hydroxylation. *Acta Crystallogr. D Biol. Crystallogr.,* 70 (2014), pp. 2875–2889

[32] W. Tempel, I. Grabovec, F. MacKenzie, Y.V. Dichenko, S.A. Usanov, A.A. Gilep, H.W. Park, N. Strushkevich. Structural characterization of human cholesterol 7alpha-hydroxylase. J*. Lipid Res.,* 55 (2014), pp. 1925–1932

[33] N. Mast, A.J. Annalora, D.T. Lodowski, K. Palczewski, C.D. Stout, I.A. Pikuleva. Structural basis for three-step sequential catalysis by the cholesterol side chain cleavage enzyme CYP11A1. *J. Biol. Chem.,* 286 (2011), pp. 5607–5613

[34] N. Strushkevich, F. MacKenzie, T. Cherkesova, I. Grabovec, S. Usanov, H.W. Park. Structural basis for pregnenolone biosynthesis by the mitochondrial monooxygenase system. *Proc. Natl. Acad. Sci. U. S. A.,* 108 (2011), pp. 10139–10143

[35] N. Strushkevich, A.A. Gilep, L. Shen, C.H. Arrowsmith, A.M. Edwards, S.A. Usanov, H.W. Park. Structural insights into aldosterone synthase substrate specificity and targeted inhibition. *Mol. Endocrinol.,* 27 (2013), pp. 315–324

[36] D. Ghosh, J. Griswold, M. Erman, W. Pangborn. Structural basis for androgen specificity and oestrogen synthesis in human aromatase. *Nature*, 457 (2009), pp. 219–223

[37] E.M. Petrunak, N.M. DeVore, P.R. Porubsky, E.E. Scott. Structures of human steroidogenic cytochrome P450 17A1 with substrates. *J. Biol. Chem.,* 289 (2014), pp. 32952–32964

[38] P.S. Pallan, L.D. Nagy, L. Lei, E. Gonzalez, V.M. Kramlinger, C.M. Azumaya, Z. Wawrzak, M.R. Waterman, F.P. Guengerich, M. Egli. Structural and kinetic basis of steroid 17alpha,20-lyase activity in teleost fish cytochrome P450 17A1 and its absence in cytochrome P450 17A2. *J. Biol. Chem.,* 290 (2015), pp. 3248–3268

[39] N. Mast, M.A. White, I. Bjorkhem, E.F. Johnson, C.D. Stout, I.A. Pikuleva. Crystal structures of substrate-bound and substrate-free cytochrome P450 46A1, the principal cholesterol hydroxylase in the brain. *Proc. Natl. Acad. Sci. U. S. A.,* 105 (2008), pp. 9546–9551

[40] T.Y. Hargrove, Z. Wawrzak, J. Liu, M.R. Waterman, W.D. Nes, G.I. Lepesheva. Structural complex of sterol 14alpha-demethylase (CYP51) with 14alpha-methylenecyclopropyl-Delta7-24, 25-dihydrolanosterol. *J. Lipid Res.,* 53 (2012), pp. 311–320

[41] K.J. McLean, P. Lafite, C. Levy, M.R. Cheesman, N. Mast, I.A. Pikuleva, D. Leys, A.W. Munro. The structure of *Mycobacterium tuberculosis* CYP125: molecular basis for cholesterol binding in a P450 needed for host infection. *J. Biol. Chem.,* 284 (2009), pp. 35524–35533

Journal of Inorganic Biochemistry, Vol 158, (May 2016): pg. 77-85. DOI. This article is © Elsevier and permission has been granted for this version to appear in e-Publications@Marquette. Elsevier does not grant permission for this article to be further copied/distributed or hosted elsewhere without the express permission from Elsevier.

***NOT THE PUBLISHED VERSION;* this is the author's final, peer-reviewed manuscript.** The published version may be accessed by following the link in the citation at the bottom of the page.

[42] J. Cupp-Vickery, R. Anderson, Z. Hatziris. Crystal structures of ligand complexes of P450eryF exhibiting homotropic cooperativity. *Proc. Natl. Acad. Sci. U. S. A.,* 97 (2000), pp. 3050–3055

[43] B. Zhao, L. Lei, N. Kagawa, M. Sundaramoorthy, S. Banerjee, L.D. Nagy, F.P. Guengerich, M.R. Waterman. Three-dimensional structure of steroid 21-hydroxylase (cytochrome P450 21A2) with two substrates reveals locations of disease-associated variants. *J. Biol. Chem.,* 287 (2012), pp. 10613–10622

[44] P.J. Mak, M.C. Gregory, S.G. Sligar, J.R. Kincaid. Resonance Raman spectroscopy reveals that substrate structure selectively impacts the heme-bound diatomic ligands of CYP17. *Biochemistry*, 53 (2014), pp. 90–100

[45] P.J. Mak, S.C. Im, H. Zhang, L.A. Waskell, J.R. Kincaid. Resonance Raman studies of cytochrome P450 2B4 in its interactions with substrates and redox partners. *Biochemistry*, 47 (2008), pp. 3950–3963

[46] T.-j. Deng, L.M. Proniewicz, J.R. Kincaid, H. Yeom, I.D.G. Macdonald, S.G. Sligar. Resonance Raman studies of cytochrome P450BM3 and its complexes with exogenous ligands. *Biochemistry*, 38 (1999), pp. 13699–13706

[47] P.J. Mak, D. Kaluka, M.E. Manyumwa, H. Zhang, T. Deng, J.R. Kincaid. Defining resonance Raman spectral responses to substrate binding by cytochrome P450 from *Pseudomonas putida. Biopolymers*, 89 (2008), pp. 1045–1053

[48] K. Matsuura, S. Yoshioka, T. Tosha, H. Hori, K. Ishimori, T. Kitagawa, I. Morishima, N. Kagawa, M.R. Waterman. Structural diversities of active site in clinical azole-bound forms between sterol 14alpha-demethylases (CYP51s) from human and *Mycobacterium tuberculosis. J. Biol. Chem.,* 280 (2005), pp. 9088–9096

[49] G.K. Jennings, A. Modi, J.E. Elenewski, C.M. Ritchie, T. Nguyen, K.C. Ellis, J.C. Hackett. Spin equilibrium and O(2)-binding kinetics of *Mycobacterium tuberculosis* CYP51 with mutations in the histidine-threonine dyad. *J. Inorg. Biochem.,* 136 (2014), pp. 81–91

[50] W.C. Chao, J.F. Lu, J.S. Wang, H.C. Yang, H.H. Chen, Y.K. Lan, Y.C. Yu, P.T. Chou, L.H. Wang. Probing the interaction between prostacyclin synthase and prostaglandin H2 analogues or inhibitors via a combination of resonance Raman spectroscopy and molecular dynamics simulation approaches. *J. Am. Chem. Soc.,* 133 (2011), pp. 18870–18879

[51] K. Oda, Y. Yamaguchi, T. Yoshimura, K. Wada, N. Nishizono. Synthetic models related to furanocoumarin-CYP 3A4 interactions. Comparison of furanocoumarin, coumarin, and benzofuran dimers as potent inhibitors of CYP3A4 activity. *Chem. Pharm. Bull.,* 55 (2007), pp. 1419–1421

Journal of Inorganic Biochemistry, Vol 158, (May 2016): pg. 77-85. DOI. This article is © Elsevier and permission has been granted for this version to appear in e-Publications@Marquette. Elsevier does not grant permission for this article to be further copied/distributed or hosted elsewhere without the express permission from Elsevier.

***NOT THE PUBLISHED VERSION;* this is the author's final, peer-reviewed manuscript.** The published version may be accessed by following the link in the citation at the bottom of the page.

[52] E. Row, S.A. Brown, A.V. Stachulski, M.S. Lennard. Development of novel furanocoumarin dimers as potent and selective inhibitors of CYP3A4. *Drug Metab. Dispos.,* 34 (2006), pp. 324–330

[53] B. Piver, F. Berthou, Y. Dreano, D. Lucas. Differential inhibition of human cytochrome P450 enzymes by epsilon-viniferin, the dimer of resveratrol: comparison with resveratrol and polyphenols from alcoholized beverages. *Life Sci.,* 73 (2003), pp. 1199–1213

[54] K. Iwanaga, M. Hayashi, Y. Hamahata, M. Miyazaki, M. Shibano, M. Taniguchi, K. Baba, M. Kakemi. Furanocoumarin derivatives in Kampo extract medicines inhibit cytochrome P450 3A4 and P-glycoprotein. *Drug Metab. Dispos.,* 38 (2010), pp. 1286–1294

Correspondence to: S.G. Sligar, Department of Biochemistry, University of Illinois, Urbana, IL 61801, United States. Corresponding author.

Journal of Inorganic Biochemistry, Vol 158, (May 2016): pg. 77-85. DOI. This article is © Elsevier and permission has been granted for this version to appear in e-Publications@Marquette. Elsevier does not grant permission for this article to be further copied/distributed or hosted elsewhere without the express permission from Elsevier.